



PEARL

Chloride penetration in concrete with trilinear binding isotherm

Li, D; Li, P; Li, L-Y

Published in:

Journal of Building Engineering

DOI:

[10.1016/j.jobe.2023.107534](https://doi.org/10.1016/j.jobe.2023.107534)

Publication date:

2023

Link:

[Link to publication in PEARL](#)

Citation for published version (APA):

Li, D., Li, P., & Li, L.-Y. (2023). Chloride penetration in concrete with trilinear binding isotherm. *Journal of Building Engineering*, 77(0). <https://doi.org/10.1016/j.jobe.2023.107534>

All content in PEARL is protected by copyright law. Author manuscripts are made available in accordance with publisher policies. Wherever possible please cite the published version using the details provided on the item record or document. In the absence of an open licence (e.g. Creative Commons), permissions for further reuse of content should be sought from the publisher or author.



Chloride penetration in concrete with trilinear binding isotherm

Dawang Li^a, Ping Li^a, Long-yuan Li^{b,*}

^a Guangdong Provincial Key Laboratory of Durability for Marine Civil Engineering, Shenzhen University, Shenzhen, 518060, PR China

^b School of Engineering, Computing and Mathematics, University of Plymouth, Plymouth, PL4 8AA, UK

ARTICLE INFO

Keywords:

Chloride
Diffusion
Chloride binding
Concrete
Analytical solution

ABSTRACT

Chloride binding in concrete is an important factor and it can significantly affect the penetration speed of chlorides in concrete and thus the service life of concrete structures. In this paper a new chloride binding isotherm is proposed to be included in the diffusion model of chlorides in concrete. Instead of the use of the traditional Freundlich or Langmuir isotherm, the present chloride binding model uses a trilinear function to describe the chloride binding in concrete. The trilinear binding isotherm not only reflects the nonlinear binding feature of chlorides in concrete when it is exposed to a chloride environment, but also makes it possible to achieve an analytical solution of the chloride diffusion equation. In the present paper, the superior of using trilinear binding isotherm to other binding isotherms is demonstrated. The detailed derivation of the analytical solution of the chloride diffusion equation with nonlinear binding feature is described and illustrated. To demonstrate the rationality and accuracy of the analytical solution derived, comparisons between the analytical solution and the numerical solution and experimental results are also provided. It is shown that the chloride diffusion profiles obtained from the chloride diffusion equation with the trilinear binding isotherm are much closer the experimental results than that obtained from the chloride diffusion equation with linear or bilinear binding isotherm.

1. Introduction

Chloride attack is one of the major structural deterioration problems in reinforced concrete structures. Chloride-induced reinforcing steel corrosion not only reduces the load-carrying capacity of reinforcing steel bars inside of the concrete but also can lead to the cracking, delamination and/or spalling of the concrete cover. In order to predict the chloride attack-induced deterioration of reinforced concrete structures, one has to know how chlorides penetrate concrete from its surrounding environment. Currently, most of researchers and practical engineers use the ionic diffusion model to predict the chloride penetration in concrete [1–3]. However, ionic diffusion in concrete pore solution is different from the ionic diffusion in water. The former is affected not only by the porosity and tortuosity of the concrete but also the interaction between solid and liquid phases involved in concrete [4–6]. For the effect of porosity and tortuosity one can use a reduced diffusion coefficient, whereas for the interaction between solid and liquid phases one has to consider the physical and chemical reactions taking place in concrete pore structure during the ionic penetration. For chloride ions one of such reactions is the chloride binding. Although there have been numerous experimental tests on chloride binding reported in literature, the exact mechanism of chloride binding in concrete is still not well understood. This is because the chloride binding in concrete involves complicated processes and is heavily dependent on the type of cement or binder used in the concrete mixture [7–9]. Currently, the chloride binding isotherm for a given concrete type is determined empirically by using the free and total chlorides

* Corresponding author.

E-mail address: long-yuan.li@plymouth.ac.uk (L.-y. Li).

directly measured in experiments [10,11]. The total chloride is the sum of the free and bound chlorides. The chloride binding isotherm represents the relationship between the free and bound chlorides. In general, a concrete with good chloride binding ability is expected to be more resistant to chloride penetration and consequently is highly resistant to reinforcing steel corrosion. Thus, an important issue in modelling chloride transport in concrete is how to incorporate an appropriate chloride binding isotherm in the transport model to describe the penetration of chlorides in concrete [12,13].

To determine chloride binding in different types of concrete, experimental tests on cement pastes, mortars and concrete specimens with various mixtures have been carried out in last four decades. From the experimentally obtained results a number of chloride binding isotherms have been also proposed. For example, Tang and Nilsson [10] proposed a method for evaluating chloride binding capacity of concrete based on the adsorption from solution and chloride binding isotherms of ordinary Portland cement (OPC) pastes and mortars. Their experimental results showed that the relationship between free and bound chlorides could be described by the Freundlich isotherm at high free chloride concentrations and the Langmuir isotherm at low free chloride concentrations. Glass et al. [11] examined the chloride binding capacity of cement pastes in diffusion cell experiments. Spiesz et al. [14] presented a nonlinear chloride binding isotherm and the non-equilibrium conditions between free and bound chlorides in concrete for simulating rapid chloride migration tests. Baroghel-Bouny et al. [15] proposed various methods of prediction of chloride-binding isotherms of cementitious materials at equilibrium and in saturated conditions. Ye et al. [16] investigated the mechanisms of chloride binding in alkali-activated slag pastes using X-Ray diffraction (XRD) analysis, thermal gravimetric analysis (TGA), and scanning electron microscope (SEM) techniques. Avet and Scrivener [17] investigated the influence of pH value on chloride binding of plain cement and limestone calcined clay cement. Chen et al. [18] examined the influence of various phosphate corrosion inhibitors on chloride binding and release in cement pastes by using XRD and TGA techniques. Chen et al. [19] investigated the chloride binding and diffusion for cement matrix with swelling agent, early-strength agent, and set-retarding agent by using XRD, TGA, and SEM techniques. Cao et al. [20] investigated the chloride binding capacity of cement pastes immersed in chloride and various chloride-sulfate solutions. Jain et al. [21] developed chloride binding isotherms for cement hydration compounds by taking account into the effect of pH value and the presence of other ionic species. Yang et al. [22] investigated the influence of nonlinear chloride binding on the determination of chloride diffusion coefficient in concrete obtained from bulk diffusion tests. The results showed that the chloride binding isotherms in the bulk diffusion tests fitted well with the Freundlich isotherm but are not so nonlinear as expected. Teymouri et al. [23] developed the pH-dependent chloride desorption isotherms for OPC pastes exposed to $MgCl_2$, $CaCl_2$, and $NaCl$ solutions. It was shown that the Langmuir isotherm agreed well with the chloride binding of ground OPC pastes, and the amount of bound chlorides was predominantly influenced by the cation-type of chlorides in the decreasing order $CaCl_2 > MgCl_2 > NaCl$. Huang et al. [24] presented an analytical study on the diffusion of chlorides in concrete coupled with the effect of nonlinear chloride binding, in which the chloride binding was represented by using a bilinear function. Bahman-Zadeh et al. [25] presented a thermodynamic and experimental study on chloride binding of limestone containing concrete in sulfate-chloride solution. Liu et al. [26] reported the experimental and numerical studies of chloride transport and binding in concrete under the coupling of diffusion and convection. Li [27] evaluated the chloride permeability and chloride binding capacity of concrete modified with nano- SiO_2 , nano- $CaCO_3$, and multi-walled carbon nanotubes. The results demonstrate that the addition of nano- SiO_2 compromises the chloride binding capacity due to the decreased pH value of pore solution, resulting in the dissolution of Friedel's salt.

The above literature survey shows that there have been extensive studies published in literature on chloride binding in concrete. A number of chloride binding isotherms have been proposed, in which the amount of bound chlorides is expressed in terms of the concentration of free chlorides in pore solution by using a linear function with a single parameter, Freundlich's equation with two parameters, Langmuir's equation with two parameters, or a bilinear function with three parameters. When the linear or bilinear binding isotherm is used the analytical solution of the chloride diffusion equation can be achieved. However, when the Freundlich or Langmuir isotherm is used only numerical solution of the chloride diffusion equation can be obtained. Note that the linear and bilinear functions do not have wide nonlinear features and thus their application is very limited. Although the Freundlich and Langmuir isotherms provide some nonlinear features their application is also somehow limited. This is partly because the isotherm has only two parameters which restrain the variability of the function, and partly because they cannot lead to analytical solution which makes it inconvenient to do parametric study analysis. In this paper a trilinear function with five parameters is employed to describe the nonlinear binding behaviour of chlorides in concrete. The use of the trilinear function not only widens up the variability of the isotherm but also makes it possible to achieve an analytical solution of the diffusion equation. In the present study, the detailed derivation of the analytical solution of the chloride diffusion equation with trilinear binding isotherm is described and illustrated. To demonstrate the rationality and accuracy of the analytical solution derived, comparisons between the analytical solution and the numerical solution and experimental results are also provided.

2. Chloride diffusion model with chloride binding in saturated concrete

Consider the chloride diffusion in a saturated concrete. The mass conservation equation of chlorides considered in per-unit volume of concrete can be expressed as follows,

$$\frac{\partial C_T}{\partial t} = -\nabla J \quad (1)$$

where C_T is the total chloride content in per-unit volume of concrete, t is the time, and J is the flux of chlorides pass through per-unit area of concrete in per-unit time. Note that the total chloride content is the sum of free and bound chlorides, that is,

$$C_T = C_f + C_b \tag{2}$$

where C_f and C_b are the free and bound chloride contents in per-unit volume of concrete. According to Fick's first law, the flux of chlorides in Eq. (1) can be expressed as follows,

$$J = -D_{eff} \nabla \left(\frac{C_f}{\varepsilon} \right) \tag{3}$$

where D_{eff} is the effective diffusion coefficient of chlorides in concrete, ε is the porosity of the concrete, and the term C_f/ε represents the concentration of free chlorides in the pore solution. Substituting Eqs. (2) and (3) into (1), it yields,

$$\frac{\partial C_f}{\partial t} + \frac{\partial C_b}{\partial t} = \nabla \left(\frac{D_{eff}}{\varepsilon} \nabla C_f \right) \tag{4}$$

Eq. (4) indicates that, if the effective diffusion coefficient of chlorides in the concrete, the porosity of the concrete, and the relationship between the free and bound chlorides in the concrete are known, then Eq. (4) together with the initial and boundary conditions of free chlorides can be used to calculate the free chloride content in the concrete at any coordinate point at any time.

In literature several chloride binding models have been proposed, in which the bound chloride content is expressed in terms of the free chloride content by using the linear function, bilinear function, Freundlich function, or Langmuir function. The constants involved in these functions were determined based on experimentally obtained data. In the present study we use a trilinear function to describe the chloride binding. The present trilinear binding model not only has the nonlinear features of the Freundlich and Langmuir functions, but also makes it possible to achieve an analytical solution of the diffusion equation.

3. Chloride diffusion model with trilinear chloride binding in saturated concrete

Consider the concrete in which the chloride binding can be represented by using a trilinear function as shown in Fig. 1 below. When the concrete is exposed to a marine environment, chloride ions will diffuse from the environment into concrete. Assume that the concrete does not contain any initial chlorides and the concentration of chlorides on its exposed surface does not change with time. In this case the chloride profile in the concrete can be determined as follows.

Case 1. $C_s \leq C_{f1}$

$$\frac{\partial C_f}{\partial t} + \frac{\partial C_b}{\partial t} = \nabla \left(\frac{D_{eff}}{\varepsilon} \nabla C_f \right) \tag{5}$$

$$C_b(t, x) = k_1 C_f \tag{6}$$

$$C_f(0, x) = 0 \tag{7}$$

$$C_f(t, 0) = C_s \tag{8}$$

Case 2. $C_{f1} < C_s \leq C_{f2}$

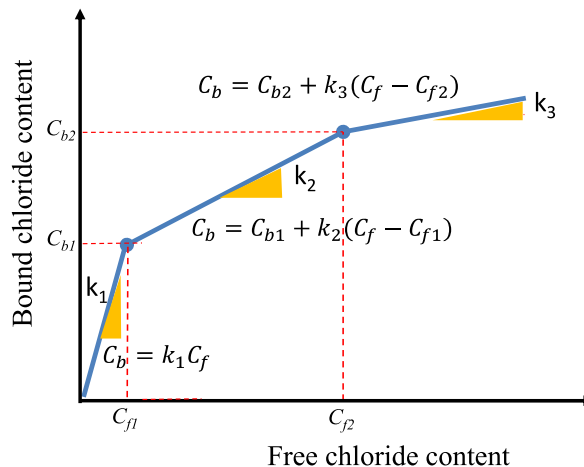


Fig. 1. Trilinear chloride binding model with five parameters.

$$\frac{\partial C_f}{\partial t} + \frac{\partial C_b}{\partial t} = \nabla \left(\frac{D_{eff}}{\varepsilon} \nabla C_f \right) \quad (9)$$

$$C_b(t, x) = \begin{cases} k_1 C_f & \text{for } C_f \leq C_{f1} \\ C_{cb1} + k_2 (C_f - C_{f1}) & \text{for } C_f > C_{f1} \end{cases} \quad (10)$$

$$C_f(0, x) = 0 \quad (11)$$

$$C_f(t, 0) = C_s \quad (12)$$

Case 3. $C_{f2} < C_s$

$$\frac{\partial C_f}{\partial t} + \frac{\partial C_b}{\partial t} = \nabla \left(\frac{D_{eff}}{\varepsilon} \nabla C_f \right) \quad (13)$$

$$C_b(t, x) = \begin{cases} k_1 C_f & \text{for } C_f \leq C_{f1} \\ C_{cb1} + k_2 (C_f - C_{f1}) & \text{for } C_{f1} < C_f \leq C_{f2} \\ C_{cb2} + k_3 (C_f - C_{f2}) & \text{for } C_f > C_{f2} \end{cases} \quad (14)$$

$$C_f(0, x) = 0 \quad (15)$$

$$C_f(t, 0) = C_s \quad (16)$$

where k_1 , k_2 and k_3 are the slopes of the chloride binding curve defined in Fig. 1, (C_{f1} , C_{b1}) and (C_{f2} , C_{b2}) are the free and bound chloride concentrations defined for different binding zones as shown in Fig. 1, C_s is the chloride concentration on the exposed surface of concrete, and x is the distance from the exposed surface. Of the seven constants (k_1 , k_2 , k_3 , C_{f1} , C_{f2} , C_{b1} , C_{b2}) involved in the trilinear chloride binding model only five are independent. These five constants can be determined based on experimentally obtained chloride binding isotherms [28–34]. After the chloride binding is defined, the chloride profile in concrete can be obtained by solving the diffusion equations defined by Eqs. (5)–(8), or (9)–(12), or (13)–(16), depending on the chloride concentration at the exposed surface of the concrete.

To demonstrate the generality and superior of the proposed trilinear chloride binding model, Fig. 2 shows a comprehensive comparison of the trilinear model and other commonly used chloride binding models with the experimental data obtained from three different types of binders: (1) the mortar mixed with water:OPC:sand ratio of 0.5:1.0:2.0, (2) the cement paste mixed by 70% OPC plus 30% fly ash (FA) with water-to-binder ratio of 0.5, and (3) the cement paste mixed by 85% OPC plus 15% silica fume (SF) with water-to-binder ratio of 0.45. The experimental data for these three binders were taken from Refs. [15,35,36], respectively. It can be seen from the figure that, for OPC binder (Fig. 2a) and OPC + FA binder (Fig. 2b) the present trilinear binding model provides the best fit to the experimental data, followed by the Freundlich and bilinear models; whereas the Langmuir model does not perform very well. For OPC + SF binder (Fig. 2c), again, the present trilinear model gives the best fit to the experimental data, whereas all other three models do not perform very well. This demonstrates that the present trilinear chloride binding model can cover a wide range of chloride binding behaviours and thus can be used to represent the chloride binding in various types of concrete.

4. Analytical solution of diffusion model with trilinear chloride binding

The trilinear chloride binding model presents the nonlinear binding behaviour of chlorides in concrete. More importantly, the use of the trilinear function makes it possible to achieve the analytical solutions defined in different binding zones. According to the diffusion equations described in the previous section, we can solve them separately based on three different cases (see Fig. 3 below).

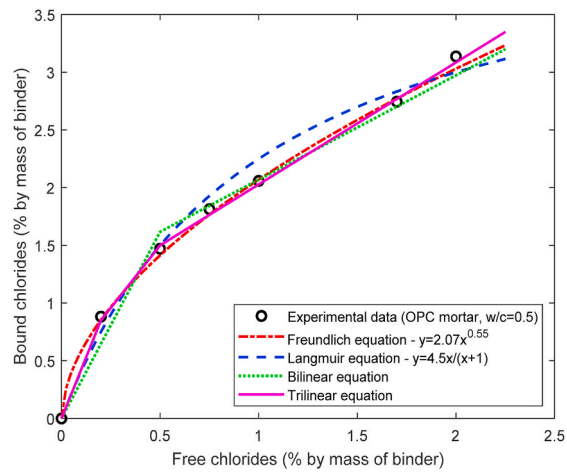
4.1. Case 1

When the surface chloride concentration C_s is not greater than C_{f1} , the chloride profile in concrete can be obtained by solving Eqs. (5)–(8), in which the bound chloride is linearly proportional to the free chloride (zone 1). In this case the diffusion equation, Eq. (5), can be simplified into,

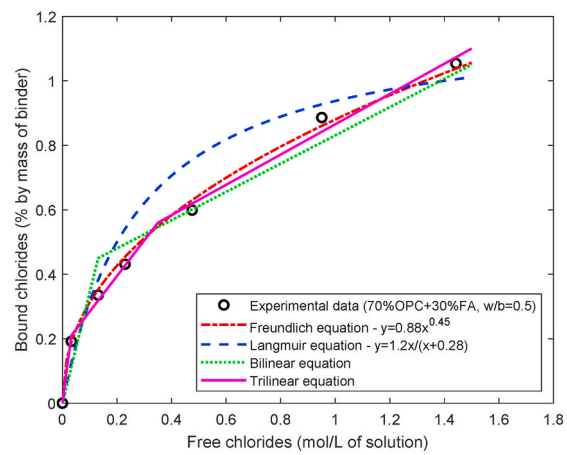
$$\frac{\partial C_f}{\partial t} = \frac{D_{eff}}{\varepsilon(1+k_1)} \nabla^2 C_f \quad (17)$$

According to the initial and boundary conditions given by Eqs. (7) and (8) and assuming $C_f(t, \infty) = 0$, the solution of Eq. (17) thus can be expressed as [37,38],

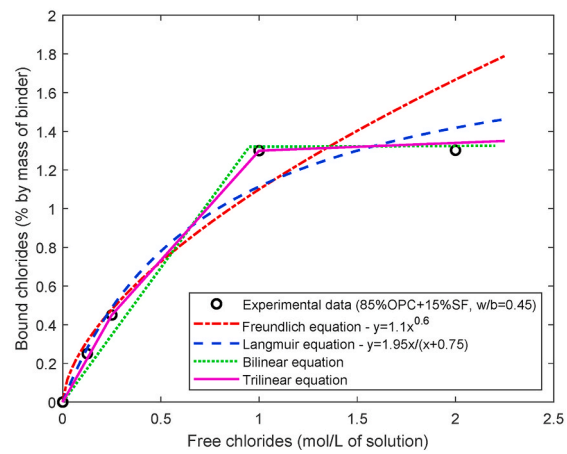
$$C_f(t, x) = C_s \left(1 - \operatorname{erf} \frac{x}{2\sqrt{D_1 t}} \right) \quad (18)$$



(a)



(b)



(c)

Fig. 2. Comparison of different chloride binding models with experimental data. (a) OPC mortar. (b) OPC + FA binder. (c) OPC + SF binder.

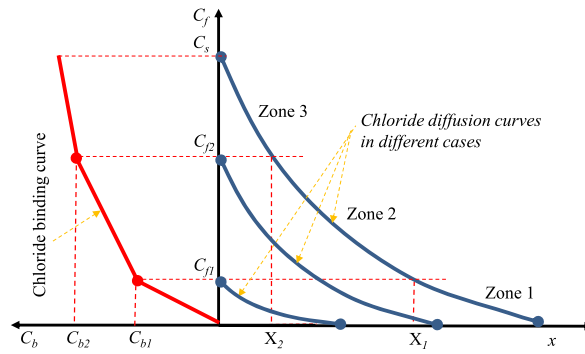


Fig. 3. Chloride diffusion in different binding zones.

where $D_1 = \frac{D_{eff}}{\varepsilon(1+k_1)}$ is the equivalent diffusion coefficient of chlorides in zone 1 where $C_f \leq C_{f1}$, and $erf(\bullet)$ is the error function.

4.2. Case 2

When the surface chloride concentration C_s exceeds C_{f1} but is not greater than C_{f2} , the chloride profile in concrete can be obtained by solving Eqs. (9)–(12), in which the bound chloride is a bilinear function of the free chloride (zone 1 and zone 2). In this case the diffusion equation, Eq. (9), can be simplified as follows,

$$\frac{\partial C_f}{\partial t} = \frac{D_{eff}}{\varepsilon(1+k_1)} \nabla^2 C_f \text{ for } C_f \leq C_{f1} \tag{19}$$

$$\frac{\partial C_f}{\partial t} = \frac{D_{eff}}{\varepsilon(1+k_2)} \nabla^2 C_f \text{ for } C_f > C_{f1} \tag{20}$$

According to the initial condition given by Eq. (11) and assuming $C_f(t, \infty) = 0$, the solution of Eq. (19) thus can be expressed as,

$$C_f^1(t, x) = A_1 \left(1 - erf \frac{x}{2\sqrt{D_1 t}} \right) \text{ for } C_f \leq C_{f1} \tag{21}$$

where A_1 is a constant to be determined. According to the initial and boundary conditions given by Eqs. (11) and (12), the solution of Eq. (20) thus can be expressed as [37,38],

$$C_f^2(t, x) = C_s - A_2 erf \frac{x}{2\sqrt{D_2 t}} \text{ for } C_f > C_{f1} \tag{22}$$

where $D_2 = \frac{D_{eff}}{\varepsilon(1+k_2)}$ is the equivalent diffusion coefficient of chlorides in zone 2 where $C_{f1} < C_f \leq C_{f2}$, and A_2 is a constant to be determined.

Let $X_1(t)$ be the coordinate point where $C_f^1(t, x) = C_f^2(t, x) = C_{f1}$. According to the continuity condition of concentration, we have the following equations,

$$C_f^1(t, X_1) = A_1 \left(1 - erf \frac{X_1}{2\sqrt{D_1 t}} \right) = C_{f1} \tag{23}$$

$$C_f^2(t, X_1) = C_s - A_2 erf \frac{X_1}{2\sqrt{D_2 t}} = C_{f1} \tag{24}$$

Solving Eqs. (23) and (24) for A_1 and A_2 , it yields,

$$A_1 = \frac{C_{f1}}{1 - erf \frac{X_1}{2\sqrt{D_1 t}}} \tag{25}$$

$$A_2 = \frac{C_s - C_{f1}}{erf \frac{X_1}{2\sqrt{D_2 t}}} \tag{26}$$

The coordinate $X_1(t)$ can be determined based on the continuity condition of flux at that point, that is,

$$-D_{eff} \nabla \left(\frac{C_f^1}{\varepsilon} \right) \Big|_{x=X_1} = -D_{eff} \nabla \left(\frac{C_f^2}{\varepsilon} \right) \Big|_{x=X_1} \tag{27}$$

Substituting Eqs. (21), (22), (25) and (26) into (27), it yields,

$$\frac{C_s - C_{f1}}{C_{f1}} \bullet \frac{1 - \operatorname{erf} \frac{X_1}{2\sqrt{D_1 t}}}{\operatorname{erf} \frac{X_1}{2\sqrt{D_2 t}}} = \sqrt{\frac{D_2}{D_1}} \exp \left[\frac{X_1^2}{4t} \left(\frac{1}{D_2} - \frac{1}{D_1} \right) \right] \quad (28)$$

Eq. (28) can be used to determine X_1/\sqrt{t} numerically. After then, A_1 and A_2 can be determined from Eqs. (25) and (26).

4.3. Case 3

When the surface chloride concentration C_s exceeds C_{f2} , the chloride profile in concrete can be obtained by solving Eqs.(13)–(16), in which the bound chloride is a trilinear function of the free chloride (zone 1, zone 2, and zone 3). In this case the diffusion equation, Eq. (13), can be simplified as follows,

$$\frac{\partial C_f}{\partial t} = \frac{D_{eff}}{\varepsilon(1+k_1)} \nabla^2 C_f \text{ for } C_f \leq C_{f1} \quad (29)$$

$$\frac{\partial C_f}{\partial t} = \frac{D_{eff}}{\varepsilon(1+k_2)} \nabla^2 C_f \text{ for } C_{f1} < C_f \leq C_{f2} \quad (30)$$

$$\frac{\partial C_f}{\partial t} = \frac{D_{eff}}{\varepsilon(1+k_3)} \nabla^2 C_f \text{ for } C_f > C_{f2} \quad (31)$$

According to the initial condition given by Eq. (15) and assuming $C_f(t, \infty) = 0$, the solution of Eq. (29) thus can be expressed as,

$$C_f^1(t, x) = A_1 \left(1 - \operatorname{erf} \frac{x}{2\sqrt{D_1 t}} \right) \text{ for } C_f \leq C_{f1} \quad (32)$$

where A_1 is a constant to be determined. According to the initial and boundary conditions given by Eqs. (15) and (16), the solution of Eq. (31) thus can be expressed as,

$$C_f^3(t, x) = C_s - A_2 \operatorname{erf} \frac{x}{2\sqrt{D_3 t}} \text{ for } C_f > C_{f2} \quad (33)$$

where $D_3 = \frac{D_{eff}}{\varepsilon(1+k_3)}$ is the equivalent diffusion coefficient of chlorides in zone 3 where $C_f > C_{f2}$, and A_2 is a constant to be determined. The solution of Eq. (30) can be expressed as [37,38],

$$C_f^2(t, x) = A_3 - A_4 \operatorname{erf} \frac{x}{2\sqrt{D_2 t}} \text{ for } C_{f1} < C_f \leq C_{f2} \quad (34)$$

where A_3 and A_4 are the constants to be determined. Let $X_1(t)$ be the coordinate point where $C_f^1(t, x) = C_f^2(t, x) = C_{f1}$, and $X_2(t)$ be the coordinate point where $C_f^2(t, x) = C_f^3(t, x) = C_{f2}$. According to the continuity condition of concentration, we have the following equations,

$$C_f^1(t, X_1) = A_1 \left(1 - \operatorname{erf} \frac{X_1}{2\sqrt{D_1 t}} \right) = C_{f1} \quad (35)$$

$$C_f^2(t, X_1) = A_3 - A_4 \operatorname{erf} \frac{X_1}{2\sqrt{D_2 t}} = C_{f1} \quad (36)$$

$$C_f^2(t, X_2) = A_3 - A_4 \operatorname{erf} \frac{X_2}{2\sqrt{D_2 t}} = C_{f2} \quad (37)$$

$$C_f^3(t, X_2) = C_s - A_2 \operatorname{erf} \frac{X_2}{2\sqrt{D_3 t}} = C_{f2} \quad (38)$$

Solving Eqs.(35)–(38) for $A_1, A_2, A_3,$ and A_4 , it yields,

$$A_1 = \frac{C_{f1}}{1 - \operatorname{erf} \frac{X_1}{2\sqrt{D_1 t}}} \quad (39)$$

$$A_2 = \frac{C_s - C_{f2}}{\operatorname{erf} \frac{X_2}{2\sqrt{D_3 t}}} \quad (40)$$

$$A_3 = \left(\frac{C_{f1}}{\operatorname{erf} \frac{X_1}{2\sqrt{D_2 t}}} - \frac{C_{f2}}{\operatorname{erf} \frac{X_2}{2\sqrt{D_2 t}}} \right) \left(\frac{1}{\operatorname{erf} \frac{X_1}{2\sqrt{D_2 t}}} - \frac{1}{\operatorname{erf} \frac{X_2}{2\sqrt{D_2 t}}} \right)^{-1} \quad (41)$$

$$A_4 = \frac{C_{f1} - C_{f2}}{\operatorname{erf} \frac{X_2}{2\sqrt{D_2t}} - \operatorname{erf} \frac{X_1}{2\sqrt{D_2t}}} \tag{42}$$

The coordinate $X_1(t)$ and $X_2(t)$ can be determined based on the continuity conditions of flux at these two points, that is,

$$-D_{\text{eff}} \nabla \left(\frac{C_f^1}{\varepsilon} \right) \Big|_{x=X_1} = -D_{\text{eff}} \nabla \left(\frac{C_f^2}{\varepsilon} \right) \Big|_{x=X_1} \tag{43}$$

$$-D_{\text{eff}} \nabla \left(\frac{C_f^2}{\varepsilon} \right) \Big|_{x=X_2} = -D_{\text{eff}} \nabla \left(\frac{C_f^3}{\varepsilon} \right) \Big|_{x=X_2} \tag{44}$$

Substituting Eqs.(32)–(34) and (39)–(42) into (43) and (44), it yields,

$$\frac{C_{f1} - C_{f2}}{C_{f1}} \cdot \frac{1 - \operatorname{erf} \frac{X_1}{2\sqrt{D_1t}}}{\operatorname{erf} \frac{X_2}{2\sqrt{D_2t}} - \operatorname{erf} \frac{X_1}{2\sqrt{D_2t}}} = \sqrt{\frac{D_2}{D_1}} \exp \left[\frac{X_1^2}{4t} \left(\frac{1}{D_2} - \frac{1}{D_1} \right) \right] \tag{45}$$

$$\frac{C_{f1} - C_{f2}}{C_s - C_{f2}} \cdot \frac{\operatorname{erf} \frac{X_2}{2\sqrt{D_3t}}}{\operatorname{erf} \frac{X_2}{2\sqrt{D_2t}} - \operatorname{erf} \frac{X_1}{2\sqrt{D_2t}}} = \sqrt{\frac{D_2}{D_3}} \exp \left[\frac{X_2^2}{4t} \left(\frac{1}{D_2} - \frac{1}{D_3} \right) \right] \tag{46}$$

Eqs. (45) and (46) can be used to determine X_1/\sqrt{t} and X_2/\sqrt{t} numerically. After then, A_1 , A_2 , A_3 and A_4 can be determined from Eqs.(39)–(42), and thus the chloride profiles in the three different zones can be calculated using the analytical solutions given by Eqs. (32)–(34).

5. Comparisons with numerical and experimental results

To demonstrate the present analytical solution, we herein show two examples. The first example is for the chloride binding, which is similar to the Langmuir or Freundlich isotherm but is represented by the trilinear function with $k_1 > k_2 > k_3$. The second example is for a special case, in which the zone one represents the chemical binding ($k_1 \rightarrow \infty$ and $C_{f1} \rightarrow 0$), the zone two is to simulate the physical binding, and the zone 3 is when the bound chloride reaches to its limit values ($k_3 \rightarrow 0$) [6]. Note that the surface chloride concentrations in these two examples are all assumed to be greater than C_{f2} (that is case 3). This is because if $C_s \leq C_{f2}$ the trilinear chloride binding model will reduce to the bilinear chloride binding model, which has been investigated previously in article [24] and thus is not discussed here again. The parametric values employed in the two examples are provided in Table 1.

Fig. 4 shows the free chloride distribution profiles at three different times, in which the analytical solution is obtained from Eqs. (32)–(34), and the numerical solution is obtained by solving Eq. (4) numerically using pdepe script built in MatLab software. It can be seen from Fig. 4 that there is almost no difference between the analytical and numerical solutions. This demonstrates that the present analytical solution is able to describe the diffusion of chlorides in concrete with different nonlinear binding features. Note that for example 2, to ensure the numerical solution obtained is accurate enough special care is required for obtaining the numerical solution because the large value of k_1 involved in the binding isotherm [39]. However, for the analytical solution it does not have this kind of issue.

The experimental validation of the present model is shown in Fig. 5, in which the experimental results were obtained from articles [24,28]. The experimental data shown in the figure are the free chlorides measured in the 120-day diffusion tests of the concrete with water-to-binder ratio of 0.45, and 10% (LP10) and 30% (LP30) limestone powder (LP) replacement to the cement. The concrete was mixed as follows: binder (cement and limestone powder) 450 kg/m³, sand 558 kg/m³, gravel 1170 kg/m³, and superplasticizer 4.5 kg/m³. The parametric values employed in the present analytical solution are given in Table 2, in which the diffusion coefficients are taken directly from article [24], and the chloride binding constants are assumed based on the chloride binding data published in article [28]. The difference in the parametric values between the two types of concrete reflects the influence of limestone on the diffusivity of the mixed concrete. It can be seen from Fig. 5 that, by using the trilinear chloride binding model, the diffusion curves obtained from the present analytical solution agree very well with the experimentally measured diffusion curves. However, if the linear or bilinear chloride binding model was used, the analytical solution would not fit well with the experimental data as it was demonstrated in article [24].

Table 1
Parametric values used in two examples.

Parameter	Example 1	Example 2
C_s (mole/l)	0.4	0.4
C_{f1}	$0.2C_s$	$0.01C_s$
C_{f2}	$0.8C_s$	$0.8C_s$
k_1	2.5	50
k_2	0.5	0.38
k_3	$k_2/3$	$k_2/100$
$D_{\text{eff}}/\varepsilon$ (m ² /s)	1.5×10^{-11}	1.5×10^{-11}

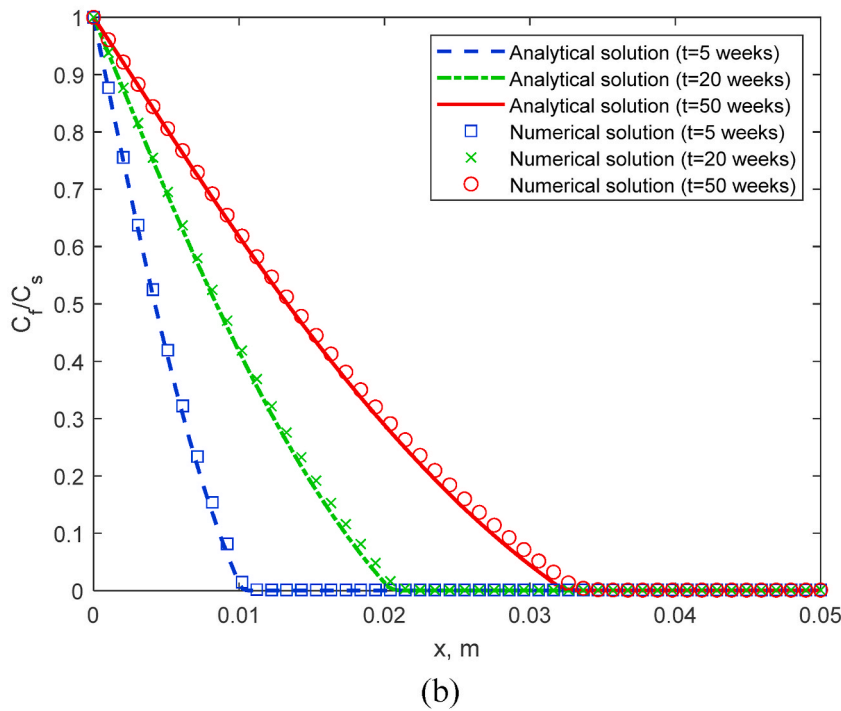
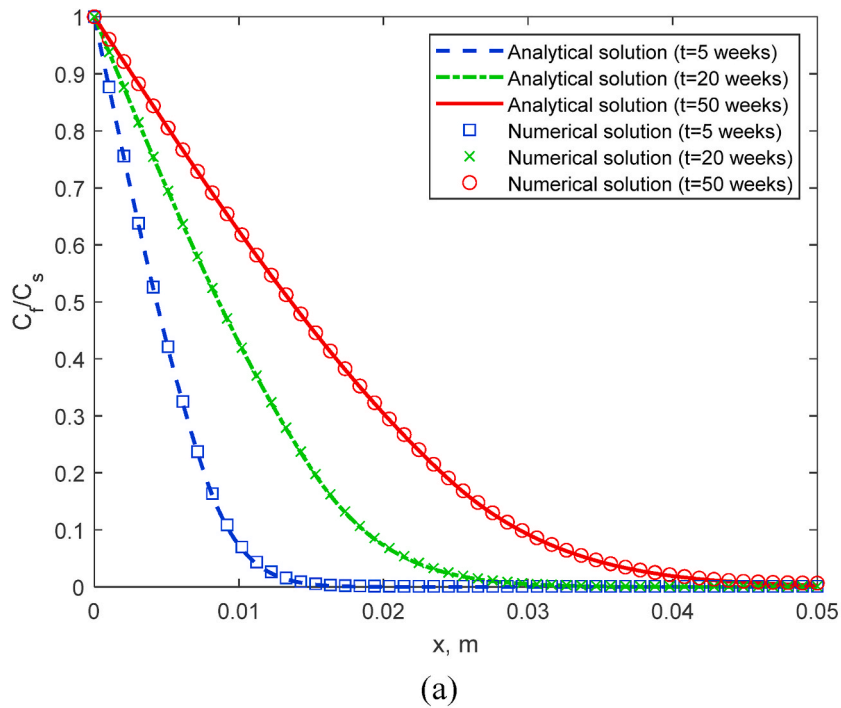


Fig. 4. Comparison of free chloride profiles between analytical and numerical solutions. (a) Example 1 and (b) example 2.

6. Conclusions

Chloring binding in concrete involves both physical and chemical reactions of chlorides with cementitious materials near the pore surface of concrete. Chloride binding can reduce the penetration speed of chlorides in concrete and thus improve the service life of concrete structures. Therefore, it is important to consider the chloride binding in the chloride diffusion model. In this paper we have proposed a trilinear chloride binding isotherm and the isotherm has been incorporated into the chloride diffusion model, from which an analytical solution is obtained. From the results and discussion presented in the paper, the following conclusions can be drawn.

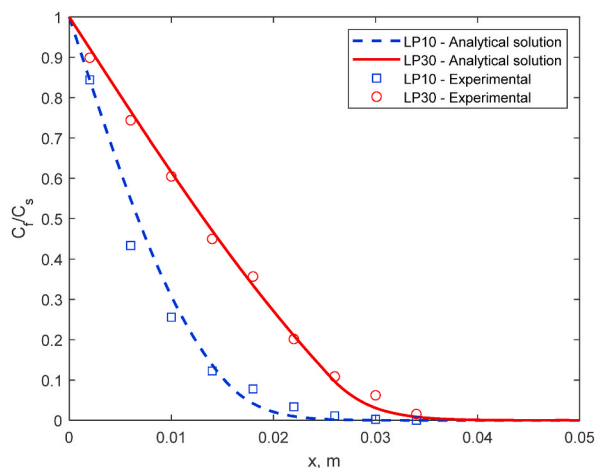


Fig. 5. Comparison of free chloride profiles between analytical solution and experimental results.

Table 2

Parametric values used in simulation of experiments.

Parameter	Concrete with 10% LP	Concrete with 30% LP
C_s (mole/l)	0.3	0.43
C_{f1}	$0.1C_s$	$0.1C_s$
C_{f2}	$0.8C_s$	$0.8C_s$
k_1	10	15
k_2	5	1
k_3	1	0.02
D_{eff}/ϵ (m^2/s)	3.32×10^{-11}	8.43×10^{-11}

- The trilinear chloride binding isotherm can effectively and efficiently represent the nonlinear binding feature of chlorides in different types of concrete.
- The analytical solution of the diffusion equation using error function, presented according to different zones is mathematically correct, which is validated by the numerical solution.
- The present analytical solution is simple and easy to use. For different types of concrete one can choose different diffusion coefficient and different chloride binding constants to describe their different diffusivities.

Declaration of competing interest

The authors declare that they have no known competing financial interests or personal relationships that could have appeared to influence the work reported in this paper.

Data availability

No data was used for the research described in the article.

Acknowledgements

The authors would like to acknowledge the financial support received from the National Natural Science Foundation of China (Grant No. 51978406, 51520105012), and the European Commission Research Executive Agency via a Marie Skłodowska-Curie Research and Innovation Staff Exchange project (H2020-MSCA-RISE-2017, TRAC-777823).

References

- [1] C.Z. Li, X.B. Song, L.H. Jiang, A time-dependent chloride diffusion model for predicting initial corrosion time of reinforced concrete with slag addition, *Cement Concr. Res.* 145 (2021), 106455, <https://doi.org/10.1016/j.cemconres.2021.106455>.
- [2] Q. Yuan, C.J. Shi, G.D. Schutter, K. Audenaert, D.H. Deng, Chloride binding of cement-based materials subjected to external chloride environment – a review, *Construct. Build. Mater.* 23 (1) (2009) 1–13, <https://doi.org/10.1016/j.conbuildmat.2008.02.004>.
- [3] M. Shafikhani, S.E. Chidiac, A holistic model for cement paste and concrete chloride diffusion coefficient, *Cement Concr. Res.* 133 (2020), 106049, <https://doi.org/10.1016/j.cemconres.2020.106049>.
- [4] D.W. Li, L.Y. Li, X.F. Wang, Chloride diffusion model for concrete in marine environment with considering binding effect, *Mar. Struct.* 66 (2019) 44–51, <https://doi.org/10.1016/j.marstruc.2019.03.004>.

- [5] D.W. Li, L.Y. Li, P. Li, Y.C. Wang, Modelling of convection, diffusion and binding of chlorides in concrete during wetting-drying cycles, *Mar. Struct.* 84 (2022), 103240, <https://doi.org/10.1016/j.marstruc.2022.103240>.
- [6] D.W. Li, X.F. Wang, L.Y. Li, An analytical solution for chloride diffusion in concrete with considering binding effect, *Ocean Eng.* 191 (2019), 106549, <https://doi.org/10.1016/j.oceaneng.2019.106549>.
- [7] M.D.A. Thomas, P.B. Bamforth, Modelling chloride diffusion in concrete: effect of fly ash and slag, *Cement Concr. Res.* 29 (4) (1999) 487–495, [https://doi.org/10.1016/S0008-8846\(98\)00192-6](https://doi.org/10.1016/S0008-8846(98)00192-6).
- [8] Y.M. Sun, M.T. Liang, T.P. Chang, Time/depth dependent diffusion and chemical reaction model of chloride transportation in concrete, *Appl. Math. Model.* 36 (3) (2012) 1114–1122, <https://doi.org/10.1016/j.apm.2011.07.053>.
- [9] J. Geng, D. Easterbrook, Q.F. Liu, L.Y. Li, Effect of carbonation on release of bound chlorides in chloride-contaminated concrete, *Mag. Concr. Res.* 68 (7) (2016) 353–363, <https://doi.org/10.1680/jmacr.15.00234>.
- [10] L.P. Tang, L.O. Nilsson, Chloride binding capacity and binding isotherms of OPC pastes and mortars, *Cement Concr. Res.* 23 (2) (1993) 247–253, [https://doi.org/10.1016/0008-8846\(93\)90089-R](https://doi.org/10.1016/0008-8846(93)90089-R).
- [11] G.K. Glass, G.M. Stevenson, N.R. Buenfeld, Chloride-binding isotherms from the diffusion cell test, *Cement Concr. Res.* 28 (7) (1998) 939–945, [https://doi.org/10.1016/S0008-8846\(98\)00071-4](https://doi.org/10.1016/S0008-8846(98)00071-4).
- [12] K. Pasupathy, J. Sanjayan, P. Rajeev, D.W. Law, The effect of chloride ingress in reinforced geopolymer concrete exposed in the marine environment, *J. Build. Eng.* 39 (2021), 102281, <https://doi.org/10.1016/j.jobte.2021.102281>.
- [13] M. Sun, C. Sun, Y. Zhang, Y. Geng, L. Fan, N. Liu, P. Zhang, J. Duan, B. Hou, Effect of carbonation curing on distribution and binding capacity of chloride ions in cement pastes, *J. Build. Eng.* 71 (2023), 106506, <https://doi.org/10.1016/j.jobte.2023.106506>.
- [14] P. Spiesz, M.M. Ballari, H.J.H. Brouwers, RCM: a new model accounting for the non-linear chloride binding isotherm and the non-equilibrium conditions between the free- and bound-chloride concentrations, *Construct. Build. Mater.* 27 (1) (2012) 293–304, <https://doi.org/10.1016/j.conbuildmat.2011.07.045>.
- [15] V. Baroghel-Bouny, X. Wang, M. Thiery, M. Saillio, F. Barberon, Prediction of chloride binding isotherms of cementitious materials by analytical model or numerical inverse analysis, *Cement Concr. Res.* 42 (9) (2012) 1207–1224, <https://doi.org/10.1016/j.cemconres.2012.05.008>.
- [16] H.L. Ye, L. Huang, Z.J. Chen, Influence of activator composition on the chloride binding capacity of alkali-activated slag, *Cement Concr. Compos.* 104 (2019), 103368, <https://doi.org/10.1016/j.cemconcomp.2019.103368>.
- [17] F. Avet, K. Scrivener, Influence of pH on the chloride binding capacity of limestone calcined clay cements (LC3), *Cement Concr. Res.* 131 (2020), 106031, <https://doi.org/10.1016/j.cemconres.2020.106031>.
- [18] Y.J. Chen, L.H. Jiang, X.C. Yan, Z.J. Song, M.Z. Guo, S.J. Zhao, W.S. Gong, Impact of phosphate corrosion inhibitors on chloride binding and release in cement pastes, *Construct. Build. Mater.* 236 (2020), 117469, <https://doi.org/10.1016/j.conbuildmat.2019.117469>.
- [19] Y.J. Chen, L.H. Jiang, X.C. Yan, Z.J. Song, M.Z. Guo, C.X. Cao, Role of swelling agent and set-controlling admixtures on chloride binding and diffusion in cement matrix, *Construct. Build. Mater.* 230 (2020), 117009, <https://doi.org/10.1016/j.conbuildmat.2019.117009>.
- [20] Y.Z. Cao, L.P. Guo, B. Chen, J.D. Wu, Thermodynamic modelling and experimental investigation on chloride binding in cement exposed to chloride and chloride-sulfate solution, *Construct. Build. Mater.* 246 (2020), 118398, <https://doi.org/10.1016/j.conbuildmat.2020.118398>.
- [21] A. Jain, B. Gencturk, M. Pirbazari, M. Dawood, A. Belarbi, M.G. Sohail, R. Kahraman, Influence of pH on chloride binding isotherms for cement paste and its components, *Cement Concr. Res.* 143 (2021), 106378, <https://doi.org/10.1016/j.cemconres.2021.106378>.
- [22] C. Yang, S.G. Wang, Y.W. Tan, C.Q. Zhang, Influence of non-linear chloride binding on the determination of apparent chloride diffusion coefficient for cement paste with mineral additives, *Construct. Build. Mater.* 308 (2021), 125017, <https://doi.org/10.1016/j.conbuildmat.2021.125017>.
- [23] M. Teymouri, M. Shakouri, N.P. Vaddey, pH-dependent chloride desorption isotherms of Portland cement paste, *Construct. Build. Mater.* 312 (2021), 125415, <https://doi.org/10.1016/j.conbuildmat.2021.125415>.
- [24] Y.Y. Huang, F.L. Ji, Z.L. Chen, J.J. Yu, Analytical solution for chloride diffusion in concrete with the consideration of nonlinear chloride binding, *Construct. Build. Mater.* 360 (2022), 129457, <https://doi.org/10.1016/j.conbuildmat.2022.129457>.
- [25] F. Bahman-Zadeh, A. Zolfagharnasab, M. Pourebrahimi, M. Mirabrishami, A.A. Ramezaniapour, Thermodynamic and experimental study on chloride binding of limestone containing concrete in sulfate-chloride solution, *J. Build. Eng.* 66 (2023), 105940, <https://doi.org/10.1016/j.jobte.2023.105940>.
- [26] Z. Liu, Y. Wang, J. Wang, C. Liu, J. Jiang, H. Li, Experiment and simulation of chloride ion transport and binding in concrete under the coupling of diffusion and convection, *J. Build. Eng.* 45 (2022), 103610, <https://doi.org/10.1016/j.jobte.2021.103610>.
- [27] C.Z. Li, Chloride permeability and chloride binding capacity of nano-modified concrete, *J. Build. Eng.* 41 (2021), 102419, <https://doi.org/10.1016/j.jobte.2021.102419>.
- [28] C.Z. Li, L.H. Jiang, The role of chloride binding mechanism in the interpretation of chloride profiles in concrete containing limestone powder, *Journal of Sustainable Cement-Based Materials* 12 (1) (2023) 24–35, <https://doi.org/10.1080/21650373.2021.2010243>.
- [29] C.Z. Li, L.H. Jiang, Effect of limestone powder addition on corrosion initiation time of reinforced concrete, *J. Build. Eng.* 59 (2022), 105132, <https://doi.org/10.1016/j.jobte.2022.105132>.
- [30] B. Martín-Pérez, H. Zibara, R.D. Hooton, M.D.A. Thomas, A study of the effect of chloride binding on service life predictions, *Cement Concr. Res.* 30 (8) (2000) 1215–1223, [https://doi.org/10.1016/S0008-8846\(00\)00339-2](https://doi.org/10.1016/S0008-8846(00)00339-2).
- [31] J. Geng, D. Easterbrook, L.Y. Li, L.W. Mo, The stability of bound chlorides in cement paste with sulfate attack, *Cement Concr. Res.* 68 (2015) 211–222, <https://doi.org/10.1016/j.cemconres.2014.11.010>.
- [32] L.B. Jin, H.L. Yu, Z. Wang, Z.Q. Wang, T. Fan, Developing a model for chloride transport through concrete considering the key factors, *Case Stud. Constr. Mater.* 17 (2022), e01168, <https://doi.org/10.1016/j.cscm.2022.e01168>.
- [33] Y.Z. Wang, C.X. Liu, Y. Tan, Y.C. Wang, Q.M. Li, Chloride binding capacity of green concrete mixed with fly ash or coal gangue in the marine environment, *Construct. Build. Mater.* 242 (2020), 118006, <https://doi.org/10.1016/j.conbuildmat.2020.118006>.
- [34] P.S. Mangat, O.O. Ojedokun, Bound chloride ingress in alkali activated concrete, *Construct. Build. Mater.* 212 (2019) 375–387, <https://doi.org/10.1016/j.conbuildmat.2019.03.302>.
- [35] T. Ishida, S. Miyahara, T. Maruya, Chloride binding capacity of mortars made with various Portland cements and mineral admixtures, *J. Adv. Concr. Technol.* 6 (2) (2008) 287–301, <https://doi.org/10.3151/jact.6.287>.
- [36] A. Babaahmadi, A. Machner, W. Kunther, J. Figueira, P. Hemstad, K. De Weerd, Chloride binding in Portland composite cements containing metakaolin and silica fume, *Cement Concr. Res.* 161 (2022), 106924, <https://doi.org/10.1016/j.cemconres.2022.106924>.
- [37] J. Crank, *The Mathematics of Diffusion*, Clarendon Press, Oxford, 1975.
- [38] D.W. Li, L.Y. Li, P. Li, F. Xing, Analytical modelling of chloride ingress in surface-treated concrete, *Ocean Eng.* 250 (2022), 111091, <https://doi.org/10.1016/j.oceaneng.2022.111091>.
- [39] L.Y. Li, P. Bettess, J.W. Bull, T. Bond, I. Applegarth, Theoretical formulations for adaptive finite element computations, *Commun. Numer. Methods Eng.* 11 (1995) 857–868, <https://doi.org/10.1002/cnm.1640111010>.